ChemPubSoc Europe

DOI: 10.1002/cctc.201402989

CHEMCATCHEM Communications

XAS and XES Techniques Shed Light on the Dark Side of Ziegler–Natta Catalysts: Active-Site Generation**

Elena Groppo,*[a] Erik Gallo,[a, b] Kalaivani Seenivasan,[a] Kirill A. Lomachenko,[a, c] Anna Sommazzi,[d] Silvia Bordiga,[a] Pieter Glatzel,[b] Roelof van Silfhout,[e] Anton Kachatkou,[e] Wim Bras,[f] and Carlo Lamberti[a, c]

The local structure and the electronic properties of the active Ti sites in heterogeneous Ziegler–Natta catalysts, generated in situ by interaction of the precatalyst with different Al-alkyl activators, were investigated by combining X-ray absorption and valence-to-core X-ray emission spectroscopy (XAS and vtc-XES), coupled with UV/Vis, FTIR, and DFT theoretical calculations. Irrespective of the activator used, the active system was found to be a highly dispersed $TiCl_3$-like phase in which the Ti sites are surrounded, not only by bridged chlorine ligands (with the same bond length of bulk $TiCl_3$), but also by terminal chlorine ligands, at a much shorter distance. These results set Ziegler–Natta catalysts in the category of complex nanomaterials. Despite the observation that the investigated catalysts polymerize ethylene, cutting-edge XAS and XES techniques do not yet offer unequivocal proof for the presence of any alkyl chain attached to the Ti sites, as a consequence of the small fraction of the active sites.

Heterogeneous Ziegler–Natta (ZN) catalysts are among the most productive and versatile catalytic systems in use in the chemical industry and are used increasingly in the polyolefin production sector (approaching 150 MTons per year)[1–6]. Their versatility can be traced to the complexity of their chemical composition. The actual generation of heterogeneous ZN catalysts consists of multiple components,[1–6] including the following: i) The active phase, which is usually a transition-metal halide of group 4 of the periodic table; ii) a poorly crystalline $MgCl_2$-based phase that increases the dispersion of the active phase; iii) electron-donor molecules, which influence the selectivity in the polymerization of α-olefins, and iv) the cocatalyst, which is usually an aluminum alkyl (such as AlR_3, R = alkyl chain). The exact role of each component and their interconnection is far from being understood, and the development of these catalysts is still more driven by trial-and-error approaches than by a rational design.[7]

One of the important, but still unanswered, questions concerns the structure (at the molecular level) of the active sites in the catalyst obtained after interaction of the precatalyst with the Al-alkyl activator. Indeed, this step is usually performed directly inside the reactor in the presence of the olefin monomer, so that the generation of the active sites is immediately followed by polymerization. According to the pioneering works of Cossee and Arlman,[8–10] the essential role of AlR_3 is the alkylation of the titanium ions where chlorine vacancies are available. Although universally accepted, this statement relies entirely on quantum chemical principles and on the crystal chemistry of transition-metal-chloride structures; direct experimental evidence of the structure of the active sites is still missing. Several reasons account for this lack of information, among which the most critical reasons are the rapid deactivation (i.e. rearrangement of the Ti–R bond, which undergoes an easy β-elimination reaction) and the small fraction of the active sites,[11] along with the difficulty in handling the AlR_3 activator. All of these problems contribute towards rendering the active sites elusive to most experimental techniques.[12] As a matter of fact, the majority of experimental data on ZN catalysts refer to the precatalyst or to aged catalysts.

Herein, we focus on a particular class of heterogeneous ZN catalysts, based on Ti and Mg chloride tetrahydrofuranates, which were patented a long time ago for polyethylene production[13] and have been recently "rediscovered" for basic studies by means of multiple experimental methods.[14–18] The specific goal is to gain insights into the electronic properties and the local structure around the Ti active sites (in terms of number and type of ligands, and of coordination distances), and to provide direct evidence (if possible) of the presence of a Ti–alkyl bond. Therefore, we combined two synchrotron-based techniques that have the advantage of being element selective:

[a] Dr. E. Groppo, Dr. E. Gallo, Dr. K. Seenivasan, K. A. Lomachenko, Prof. S. Bordiga, Prof. C. Lamberti
Department of Chemistry, INSTM and NIS Centre
Università di Torino
Via Quarello 15, 10135 Torino (Italy)
Fax: (+39) 011-6707855
E-mail: elena.groppo@unito.it

[b] Dr. E. Gallo, Dr. P. Glatzel
European Synchrotron Radiation Facility
6 Rue Jules Horowitz, 38043 Grenoble (France)

[c] K. A. Lomachenko, Prof. C. Lamberti
Southern Federal University
Zorge Street 5, 344090 Rostov-on-Don (Russia)

[d] Dr. A. Sommazzi
Versalis - Novara Research Center, Istituto Eni Donegani
Via Fauser, 4-28100 Novara (Italy)

[e] Dr. R. van Silfhout, A. Kachatkou
The University of Manchester
Sackville Street, Manchester M13 9PL (United Kingdom)

[f] Dr. W. Bras
Netherlands Organization for Scientific Research
Dubble@ ESRF, Grenoble (France)

[**] XAS = X-ray absorption spectroscopy; XES = X-ray emission spectroscopy.

Supporting Information for this article is available on the WWW under http://dx.doi.org/10.1002/cctc.201402989.

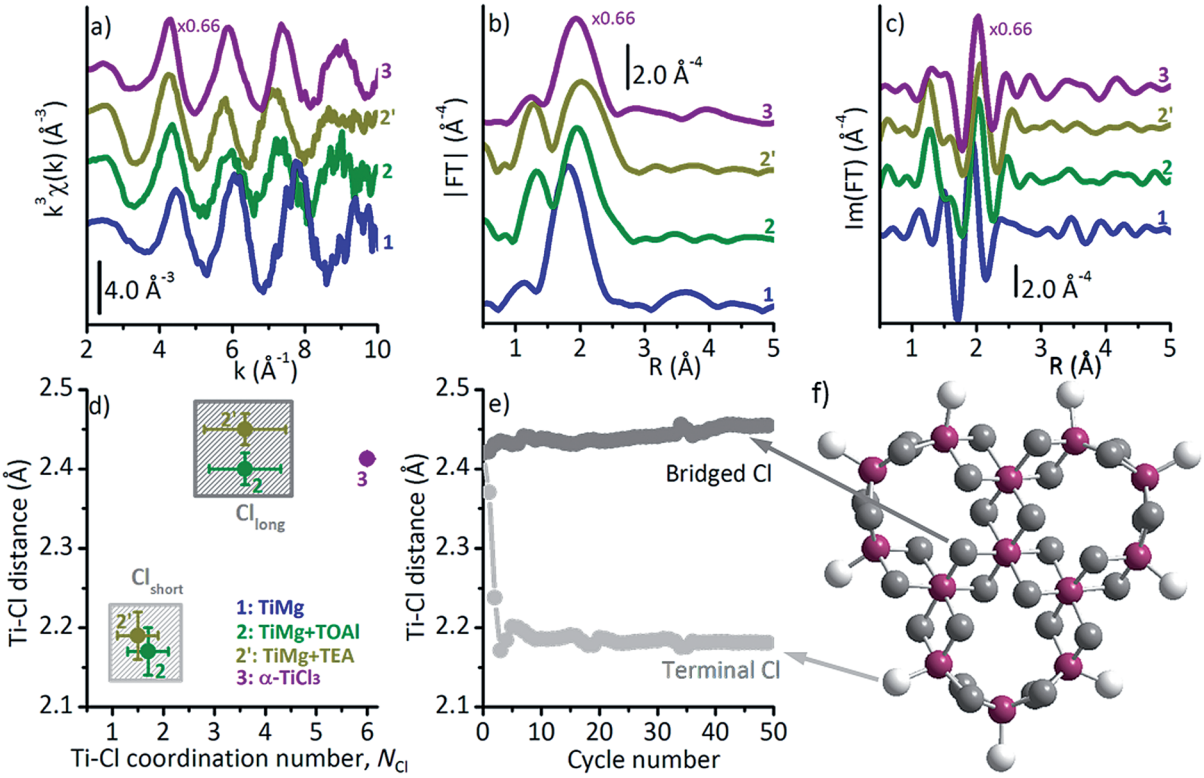

Figure 1. a–c): k^3-weighted χ(k) functions and corresponding Fourier transforms (in both modulus and imaginary parts) of the TiMg precatalyst (**1**) and of the same sample after interaction with TOAl (**2**) and TEA (**2′**). The spectrum of violet $TiCl_3$ (**3**), multiplied by a factor of 0.66, is shown for comparison. The spectra were vertically translated for clarity. d) Summary of the fitted Ti–Cl distances (Å) and of the corresponding coordination numbers (N_{Cl}), resulting from the data analysis of the EXAFS data shown in (a–c). Grey boxes highlight the contributions of two different chlorine ligands, at shorter (Cl_{short}) and longer (Cl_{long}) bond distances. e) Evolution of the Ti–Cl bond distances for central and terminal titanium atoms during the geometry optimization, carried out at the DFT level on the cluster shown in (f). Bridged chlorine, terminal chlorine, and titanium atoms are shown in dark grey, light grey and violet, respectively. Arrows indicate the bonds that were being monitored.

i) Ti K-edge X-ray absorption spectroscopy (XAS)[19,20] and ii) valence-to-core X-ray emission spectroscopy (vtc-XES).[21,22] The XAS and XES experiments were performed at the BM26A[23] and ID26 beamlines at the ESRF facility (Grenoble, France), respectively. Both measurements required challenging experimental set-ups. In particular, to overcome the experimental difficulties caused by beam drift and minute sample inhomogeneities intrinsic to XAS experiments on heterogeneous catalysts at these low X-ray energies, it was necessary to develop a feedback mechanism on the X-ray optics of BM26.[24] Moreover, because of the high photon flux adopted during vtc-XES measurements (more than 10^{12} photons per second), the samples were found to suffer from radiation damage on a fast timescale (≈10 s). To circumvent this problem, each point of the vtc-XES spectrum was collected on a different sample spot irradiated for 2 seconds, and the intensity was normalized to the total fluorescence-yields signal recorded with a solid-state detector. The micrometric size of the beam allowed us to have sufficient fresh points on the sample (1.3 cm diameter pellet) to collect a full vtc-XES spectrum. Manipulation and measurements of all the samples were performed under strictly inert conditions. Further experimental details are given in the Supporting Information. The XAS–XES data were complemented with diffuse-reflectance (DR) UV/Vis and FTIR results, as well as with DFT theoretical calculations.

The precatalyst (hereafter TiMg) was obtained by reaction of $[MgCl_2(thf)_{1.5}]$ and $[TiCl_4(thf)_2]$ precursors in THF, as reported in the Experimental Section.[14] For a Mg/Ti molar ratio equal to 2, a crystalline bimetallic adduct was formed: $[TiCl_4(thf)_2]$ removes a Cl^- ion from $[MgCl_2(thf)_{1.5}]$ to form the $[TiCl_5(thf)]^-$ anion; the counter cation is a dimeric Mg-chloride tetrahydrofuranate.[14,25,26] The local structure around the Ti atoms was elucidated by the extended X-Ray absorption fine structure (EXAFS) data (Figure 1). The Fourier transform (FT) of the k^3-weighted χ(k) function (Figure 1 a,b) is dominated by a first shell peak centered around 1.8 Å (not phase corrected), which is the result of the sum of the six single-scattering contributions deriving from the first shell ligands (i.e. 1 O belonging to the thf moiety at 2.19 ± 0.08 Å, 1 Cl at 2.28 ± 0.08 Å and 4 Cl at 2.34 ± 0.08 Å, see Section S3 of the Supporting Information for a detailed analysis). In the resulting TiMg bimetallic salt the Ti sites have a +4 oxidation state and show a six-fold coordination,[12] as monitored by DR UV/Vis, X-ray absorption near-edge structure (XANES), and Kβ-XES spectroscopy (Figure 2). In particular, i) the intense absorption around 25 000 cm^{-1} in the DR UV/Vis spectrum (Figure 2 a) is assigned to fully allowed Cl(p)→Ti(d)

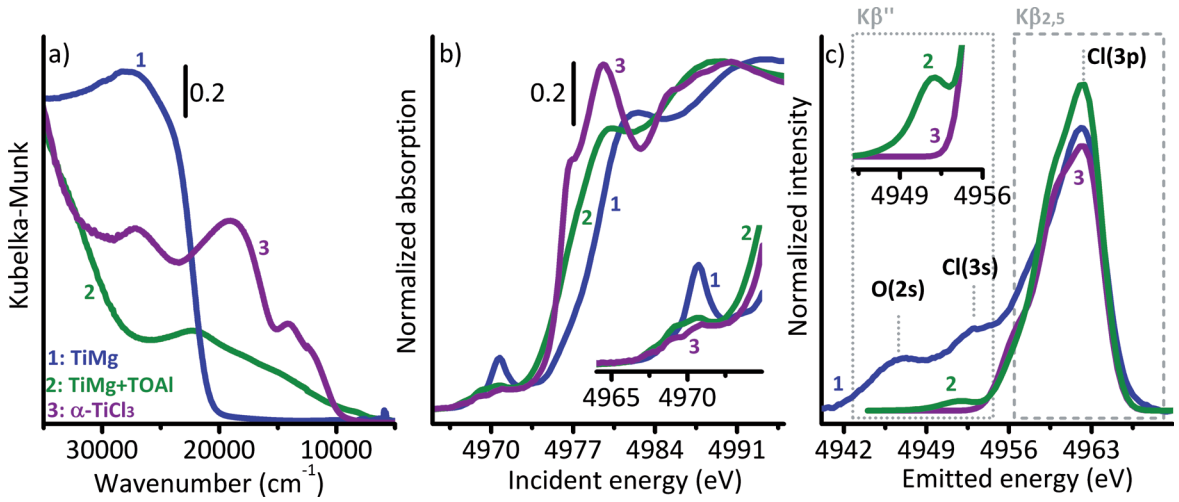

Figure 2. a) Diffuse-reflectance UV/Vis (in Kubelka–Munk units), b) normalized Ti K-edge XANES, and c) normalized vtc-XES spectra of the TiMg precatalyst (**1**) and of the catalyst obtained after interaction of TiMg with excess of TOAl (**2**). The spectra of violet $TiCl_3$ are also shown for comparison (**3**). Inset in (b) shows a magnification of the pre-edge region in the XANES spectra. Inset in (c) shows a magnification of spectra **2** and **3** in the 4950–4956 eV region. The main peaks in the vtc-XES spectra are also assigned. The Kβ″ and $K\beta_{2,5}$ regions are indicated by grey boxes.

ligand-to-metal charge-transfer transitions, in which the excited electron is associated with one of the nearest Cl^- anions and the transferred electron goes into a 3d orbital of the Ti^{4+} ion;[14,27–30] ii) the weak pre-edge peak at 4970.6 eV (shoulder at 4968.3 eV) in the XANES spectrum (Figure 2b), that precedes the absorption edge at 4979 eV, is due to 1 s→pd transitions;[14,31–34] iii) the two Kβ″ lines present in the vtc-XES spectrum (Figure 2c) at 4947 and 4953 eV are due to transitions mainly involving molecular orbitals having primarily O(2 s) and Cl(3 s) character, and thus identify the presence of oxygen and chlorine ligands in the first coordination sphere of the Ti sites.[35–37]

The catalysts were obtained from the above-mentioned precatalyst upon interaction with the AlR_3 activator. To limit catalyst deactivation, excess AlR_3 was used, and this step was performed immediately before the spectroscopic measurements. In some cases triethylaluminum (TEA, Aldrich, pure) was used, in others trioctylaluminum (TOAl, Aldrich, 25% diluted in heptane) was used. As proof that the obtained catalyst is active in ethylene polymerization, Figure 3 shows the FTIR spectrum (collected in attenuated-total-reflection mode) of TiMg + TEA after polymerization of C_2D_4 at room temperature. Deuterated ethylene was used to clearly detect the presence of polyethylene by IR spectroscopy, without interfering with the vibrational modes of the AlR_3 activator. The spectrum, dominated by the IR absorption bands of TEA and residual tetrahydrofuran, clearly shows the characteristic $\nu(CD_2)$ bands of deuterated polyethylene at 2193 and 2088 cm^{-1} (inset in Figure 3).

The effects of Al-alkyls on the precatalyst are remarkable, and involve both the local structure, as revealed by EXAFS (Figure 1) and the electronic properties, as detected by DR UV/Vis, XANES, and vtc-XES (Figure 2). EXAFS spectra of the two catalysts obtained after interaction of TiMg with TOAl and TEA (Figure 1a) are substantially different from that of TiMg. This observation provides evidence that AlR_3 causes a drastic structural change in the precatalyst. This finding is valid not only for the $MgCl_2$ phase, as previously demonstrated by X-ray powder diffraction (XRPD),[14,25] but also for all the Ti species, whose structure can not be elucidated by XRPD because of the absence of a long-range order. The effect is the same irrespective of the activator used. Moreover, the spectra of the catalysts are very similar to that of violet $TiCl_3$, although 1/3 less intense, suggesting that the local structure of the new Ti phase is analogous to that of $TiCl_3$. A closer inspection of the FT of the k^3-weighted $\chi(k)$ functions (Figure 1b,c) reveals that the first shell signal is split into two components, evidenced as a beat at 1.6 Å in the Im(FT). The additional contribution at low distance values might be due to a carbon atom belonging to an alkyl chain, in agreement with the postulated Cossee–Arlman mechanism.[8–10] Unfortunately, any attempt to fit the experimental spectrum with a Ti–C contribution yielded unsatisfactory results (see Section S4 of the Supporting Information). Instead, good results were obtained by considering that two types of chlorine ligands, at shorter ($Ti–Cl_{short}$) and longer ($Ti–Cl_{long}$) distances, exist and contribute to define the coordination sphere around the Ti sites.

A summary of the fitted Ti–Cl distances and of the corresponding coordination numbers (N_{Cl}) is shown in Figure 1d. Coordination numbers of approximately 5.3 for TiMg + TOAl and 5.1 for TiMg + TEA were obtained, compared with 6.0 for violet $TiCl_3$. Coordination numbers smaller than the reference indicate that a fraction of the Ti atoms (those at the surface) do have at least one vacancy in their coordination sphere (i.e. a fraction of Ti atoms have less than six chlorine ligands). Within the experimental error, the $Ti–Cl_{long}$ distances were found to vary in the range of 2.40–2.50 Å, and are slightly shorter for the catalyst prepared with TOAl than with TEA (appreciable also in the rough FT data, Figure 1a,b). It is worth noting that the characteristic Ti–Cl distance for bridged chlorine ligands in violet bulk $TiCl_3$ is 2.42 Å, whereas in bulk $TiCl_2$ it increases to 2.50 Å. Therefore, the longer $Ti–Cl_{long}$ distance found for TiMg + TEA catalysts suggests the presence of Ti^{2+}

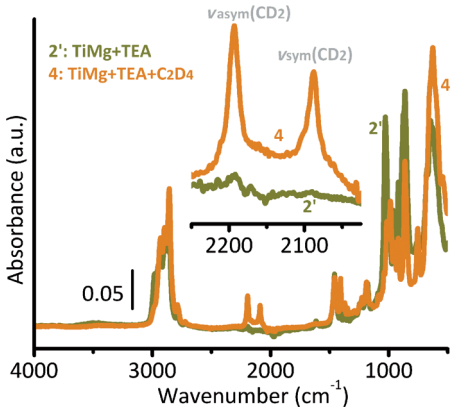

Figure 3. IR spectra, collected in ATR mode, of the TiMg + TEA catalyst before and after polymerization of C_2D_4. The inset shows a magnification of the $\nu(CD_2)$ absorption bands.

species, in agreement with the XANES and DR UV/Vis results (see below).

Additional chlorine ligands at a distance shorter ($Ti–Cl_{short}$) than that characteristic of bridged chlorine ligands in violet $TiCl_3$ characterize the Ti coordination sphere in the two catalysts. Similar results have been previously reported for similar systems ($TiCl_3/MgCl_2$[33] and $TiCl_4/MgCl_2$ + TEA[38]), although with small coordination numbers. In these works,[33,38] the short Ti–Cl distances were interpreted in terms of close interaction of the highly dispersed $TiCl_3$ phase with the $MgCl_2$ phase, which occurs through a bridged chlorine species. However, we noticed that Ti–Cl distances of approximately 2.20 Å are characteristic of terminal chlorine ligands.

We carried out a DFT geometry optimization (Figure 1e) of a $TiCl_3$ nanocluster containing 13 Ti and 39 Cl atoms (Figure 1f); the cluster was cut from the α-$TiCl_3$ bulk structure with $R\bar{3}$ symmetry reported by Troyanov et al.[39] D_3 symmetry for the cluster was enforced, mimicking the symmetry of the bulk material. One chlorine ligand was removed for each Ti atom at the border, to maintain the $TiCl_3$ stoichiometry and to simulate the presence of coordination vacancies. No other restrictions were imposed. In the initial model all the Ti–Cl distances were equal to 2.42 Å. However, in course of optimization the Ti–Cl distances evolved differently for bridged and terminal chlorine ligands (Figure 1e). Chlorine ligands bonded to the central (bulk-like) Ti atom were not significantly shifted compared to the initial positions; the resulting Ti–Cl bond length was 2.45 Å. On the contrary, for terminal chlorine ligands the Ti–Cl distances were significantly contracted compared to the bulk ones; optimization yielded the values of 2.20 ± 0.01 Å depending on the terminal Ti site. It is worth noting that virtually the same results were obtained for a cluster fully terminated with chlorine ligands. Hence, the Ti–Cl distances do not seem to be affected by the presence of a vacancy around the terminal titanium sites. The simple cluster shown in Figure 1f does not have the ambition to represent the active $TiCl_x$ phase in the investigated catalyst. For example, it does not take into account the presence of the $MgCl_2$ phase that is surely involved in the definition of the active phase. In this respect, it must be noted that Cl ligands bridged to one Mg and one Ti instead of two Ti atoms are expected to have very similar Ti–Cl distances. Nevertheless, this simple cluster allows interpretation of the EXAFS data. In particular, the following statements can be safely made: 1) The AlR_3 activators transform the molecularly well-defined TiMg precursor into a $TiCl_x$ phase having a local structure very similar to that of violet $TiCl_3$, but a much larger fraction of terminal chlorine ligands, as a consequence of reduced dimensions; 2) the terminal Cl ligands are characterized by a much shorter Ti–Cl distance; and 3) at least a fraction of the Ti sites do have a coordination vacancy.

Regarding the electronic properties, in the DR UV/Vis spectra (Figure 2a and Figure S5a), a broad absorption appears in the visible region, which is typical of d–d transition for Ti^{3+} species in a six-fold geometry.[12] Simultaneously, the intense absorption around 25000 cm^{-1} shifts upward, as expected for a decrease in the Ti oxidation state. In the XANES spectra, the edge shifts to lower energy (Figure 2b and Figure S5b), suggesting that the Ti oxidation state is less than +4.[12] The pre-edge peak becomes less intense and structured into three bands at 4967, 4969, and 4971 eV (inset in Figure 2b). Finally, the vtc-XES spectrum of the catalyst (Figure 2c) no longer shows the Kβ" lines characteristic of oxygen and chlorine ligands. Taken all together, these data provide evidence that AlR_3 reduces Ti^{4+} sites (mainly to Ti^{3+} for TOAl, and perhaps to a mixture of Ti^{3+} and Ti^{2+} for TEA), in agreement with literature results.[11] The EXAFS, DR UV/Vis, XANES, and vtc-XES spectra of the catalysts have strong similarities with the spectra of violet $TiCl_3$ (spectra **3** in Figure 2), with some differences that are discussed in the following:

1) In the UV/Vis spectrum of the catalysts (Figure 1a and Figure S5a), the intense band higher than 30000 cm^{-1} with pure ligand-to-metal charge-transfer character, is the same as that of $TiCl_3$. On the contrary, the spectra of the catalysts differ from that of $TiCl_3$ in the visible range, where the absorption bands are less intense and broader. In this respect, it should be noted that for $TiCl_3$ the assignment of the absorption bands in the 12500–14000 cm^{-1} region (Jahn–Teller split d–d transitions of Ti^{3+} sites in a distorted six-fold geometry) and higher than 30000 cm^{-1} (fully allowed charge transfer p–d transitions) is firmly established.[30,40,41] However, the nature of the bands at approximately 19000 and 27000 cm^{-1}, with an intensity between that of localized d–d transitions and that of charge-transfer transitions, has been a matter of discussion in the literature. Absorption bands in this region are characteristic of many $3d^1$ and $3d^2$ transition-metal halides, and often overlap to produce a relatively unstructured absorption that is responsible for a prevalence of black materials. The most common interpretation is that they are due to inter-site hopping transitions of the type $2(3d^1) \rightarrow 3d^0 + 3d^2$, involving couples of Ti sites bridged by chlorine ligands.[40,41] The much lower intensity of these bands in the UV/Vis spectrum of the catalyst might be an indication that they are mainly due to localized (intra-site) rather than inter-site d–d transitions. This

implies that, although bridged by chlorine ligands (as revealed by the charge-transfer band higher than 30000 cm^{-1}), the reduced Ti sites in the catalyst do not "communicate" to each other. On the other hand, the broadness of the bands in the visible region reflects a larger heterogeneity of sites. Both conclusions (more localized transitions and heterogeneity) are in agreement with the hypothesis of a $TiCl_x$ phase having reduced dimension.

2) In the XANES spectrum of the catalyst (Figure 2b and Figure S5b), the pre-edge features (which are due to localized transitions) overlap well with those of $TiCl_3$. On the contrary, the XANES spectrum of $TiCl_3$ has a much more structured edge than that of the catalyst. In particular, a sharp feature is observed at 4980 eV (with a shoulder at 4977 eV), which was assigned to allowed Ti(1s)→Cl(4p) transitions, enhanced by the multiple scattering contributions characteristic of crystalline materials.[32,33,42] These features are absent in the XANES spectrum of the catalyst, suggesting that the multiple scattering contributions are limited. This observation is again in favor of a low-dimensional $TiCl_x$ phase.
3) Finally, the vtc-XES spectrum of the catalyst and of violet $TiCl_3$ show very similar $K\beta_{2,5}$ lines (Figure 1c), which are due to transitions involving molecular orbitals with mainly a ligand p character.[43,44] Hence, the new $TiCl_x$ phase formed in the catalyst should have the same valence orbitals as violet $TiCl_3$. On the contrary, a weak peak at approximately 4952 eV is observed in the vtc-XES spectrum of the catalyst (inset in Figure 1c), which is not present in that of $TiCl_3$. In principle, transitions involving Cl(3s) molecular orbitals could contribute in this energy region (as indicated by the label for the TiMg precatalyst), provided that they also have a Ti p contribution.[35,36,45] Also, C ligands with sp^3 hybridization can contribute in the same energy region. As an example, the vtc-XES spectrum of TiC (Figure S6) shows a prominent band at 4954 eV, which identifies the sp^3-hybridized carbon ligands. Hence, the weak band at 4952 eV observed in the vtc-XES spectrum of the catalyst might identify both chlorine and carbon ligands. We tried to discriminate between the two possibilities by DFT theoretical calculations conducted on the same $TiCl_3$ nanocluster adopted to validate the EXAFS data analysis (Figure 1f). However, simulation of the XES of $TiCl_3$ was very challenging, in line with the results reported in the study of Sementa et al.,[46] and no decisive conclusions could be drawn from them. Therefore, at the present stage, we are not able to unequivocally assign the weak band at 4952 eV observed in the vtc-XES spectrum of TiMg treated in excess of TOAl.

In summary, the experimental and theoretical data discussed above contributes to the understanding of the role of aluminum alkyls in Ziegler–Natta catalysis. It was found that AlR_3 activators reduce the Ti^{4+} sites originally present in the precatalyst, mainly to Ti^{3+} for TOAl, and probably to a mixture of Ti^{3+} and Ti^{2+} for TEA. The well-defined molecular structure of the TiMg precatalyst is completely destroyed by the activators, and a new highly dispersed $TiCl_3$-like phase is formed, in which the Ti sites are quite heterogeneous. Indeed, as a consequence of the limited particle size, the Ti sites are surrounded not only by bridged chlorine ligands (with the same bond distance of bulk $TiCl_3$), but also by terminal chlorine ligands, at a much shorter distance. Moreover, a consistent fraction of the Ti sites contain a vacancy in the coordination sphere. The high dispersion of the active $TiCl_3$-like phase is testified by the observation that electronic transitions involving d electrons are more localized than for bulk $TiCl_3$. Despite the observation that the investigated catalysts polymerize ethylene, at present XAS and XES techniques do not offer unequivocal proof of the presence of any alkyl chain (i.e. carbon ligand) attached to the Ti sites. This might be an indication that the number of Ti sites carrying the alkyl chain (i.e. the active sites in ethylene polymerization) is too small a fraction of the total Ti sites, and thus below the detection sensitivity of the adopted techniques. Even though the active Ti–alkyl sites were not unequivocally identified, it was experimentally observed that the active phase originates from an extensive reconstruction of a well-defined TiMg precatalyst, and it is composed of $TiCl_3$-like nanoclusters (terminating with chlorine ligands with Ti—Cl bond distances much shorter than in the bulk). This finding potentially has many implications for the more common Ziegler–Natta catalysts obtained from the activation of the much less-defined $MgCl_2/TiCl_4$ precatalysts, for which an even larger $TiCl_x$ dispersion could be predicted. Hence, these results definitely set Ziegler–Natta catalysts in the category of complex nanomaterials, which is not yet completely recognized in the literature. In this respect, any attempt to optimize these systems should start from the awareness that they need to be treated with adequate experimental and theoretical tools. Finally, it should be noted that the problems encountered in this work are common to most heterogeneous catalysts; hence, the strategies here followed can offer some hints for the investigation of other catalytic systems.

Experimental Section

The TiMg precatalyst was synthesized by dissolving the $[TiCl_4(thf)_2]$ and $[MgCl_2(thf)_{1.5}]$ precursors separately in thf, followed by mixing both solutions (Mg/Ti = 2:1) and stirring for 3 h at room temperature. The solid product was recovered by evaporation of the solvent, washed with dry pentane, and dried under vacuum. The yellow solid obtained gave the following elemental analysis: Ti 5.9%; Mg 6.4%; Cl 32.4%.[14] The catalysts were obtained from the above-mentioned precatalyst upon interaction with the AlR_3 activator, as discussed above.

Ti K-edge XAS and vtc-XES spectra were collected at the BM26A (DUBBLE) and ID26 beamlines at the European Synchrotron Radiation Facility (ESRF, Grenoble, France), respectively. For both XAS and vtc-XES experiments, the samples were measured in the form of self-supporting pellets after mixing the powder with paraffin (transparent to X-ray), inside a homemade quartz cell equipped with two kapton windows. All the samples were manipulated in a controlled atmosphere, inside an argon-filled glove-box. Argon was removed from the cell before the measurement because it absorbs a high fraction of the incoming beam at the low energy of Ti K-edge. Further experimental details are given in the Supporting Information.

UV/Vis–NIR spectra were collected in diffuse reflectance mode on a Cary5000 Varian spectrophotometer. All the samples were measured in powdered form (diluted in Teflon) inside a cell with an optical window (suprasil quartz) and allowing measurements to be performed in a controlled atmosphere. IR spectra were collected on a Bruker Alpha instrument, equipped with an attenuated total reflection (ATR) accessory (diamond crystal), and placed inside the glove-box. The spectra were collected in the 4000–500 cm^{-1} wavenumber region, at a resolution of 2 cm^{-1}.

DFT calculations were carried out by using ADF2013 code.[47,48] Perdew–Burke–Ernzerhof exchange-correlation functional[49] combined with D3 Grimme dispersion correction[50] was used. Slater-type basis sets were chosen for all atoms: TZ2P for chlorine and TZ2P+ with additional d orbitals for titanium.[51] Relativistic effects were dealt with employing ZORA approach.[52] Frozen-core approximation was used, thus neglecting the changes occurring to core orbitals (up to 2p for both Ti and Cl) upon the formation of chemical bonds. Convergence criteria were set to 0.001 Hartree for energy, 0.001 Hartree/Å for gradients, and 0.01 Å for bond distances.

Acknowledgements

Prof. A. Zecchina is gratefully acknowledged for his constant support, everyday encouragement, and indispensable suggestions. We thank H. Müller (Chemical Lab at ESRF) for giving us access to the always perfect glove-box during the experiments at ESRF. This work was supported by "Progetti di Ricerca di Ateneo-Compagnia di San Paolo-2011-Linea 1", ORTO11RRT5 project. C.L. and K. A. L. thank the Mega-grant of the Russian Federation Government to support scientific research at Southern Federal University, No.14.Y26.31.0001.

Keywords: EXAFS spectroscopy · heterogeneous catalysis · titanium · X-ray absorption spectroscopy · Ziegler–Natta catalysts

[1] E. Albizzati, U. Giannini, G. Collina, L. Noristi, L. Resconi in *Polypropylene Handbook* (Ed.: E. P. J. Moore), Hanser-Gardner Publications, Cincinnati, **1996**, Chap. 2.
[2] R. Mülhaupt, *Macromol. Chem. Phys.* **2003**, *204*, 289–327.
[3] L. L. Böhm, *Angew. Chem. Int. Ed.* **2003**, *42*, 5010–5030; *Angew. Chem.* **2003**, *115*, 5162–5183.
[4] G. Wilke, *Angew. Chem. Int. Ed.* **2003**, *42*, 5000–5008; *Angew. Chem.* **2003**, *115*, 5150–5159.
[5] P. Corradini, G. Guerra, L. Cavallo, *Acc. Chem. Res.* **2004**, *37*, 231–241.
[6] V. Busico, *MRS Bull.* **2013**, *38*, 224–228.
[7] V. Busico, *Dalton Trans.* **2009**, 8794–8802.
[8] P. Cossee, *J. Catal.* **1964**, *3*, 80–88.
[9] E. J. Arlman, *J. Catal.* **1964**, *3*, 89–98.
[10] E. J. Arlman, P. Cossee, *J. Catal.* **1964**, *3*, 99–104.
[11] Y. V. Kissin, *Alkene Polymerization Reactions with Transition Metal Catalysts, Vol. 173*, Elsevier, Amsterdam, **2008** .
[12] E. Groppo, K. Seenivasan, C. Barzan, *Catal. Sci. Technol.* **2013**, *3*, 858–878.
[13] U. Giannini, E. Albizzati, S. Parodi, F. Pirinoli, US Patent, 4,124,532, **1978**.
[14] K. Seenivasan, A. Sommazzi, F. Bonino, S. Bordiga, E. Groppo, *Chem. Eur. J.* **2011**, *17*, 8648–8656.
[15] E. Grau, A. Lesage, S. Norsic, C. Copéret, V. Monteil, P. Sautet, *ACS Catal.* **2013**, *3*, 52–56.
[16] W. Phiwkliang, B. Jongsomjit, P. Praserthdam, *J. Appl. Polym. Sci.* **2013**, *130*, 1588–1594.
[17] S. Ntais, A. Siokou, *Surf. Sci.* **2006**, *600*, 4216–4220.
[18] S. Ntais, V. Dracopoulos, A. Siokou, *J. Mol. Catal. A* **2004**, *220*, 199–205.
[19] S. Bordiga, E. Groppo, G. Agostini, J. A. Van Bokhoven, C. Lamberti, *Chem. Rev.* **2013**, *113*, 1736–1850.
[20] L. Mino, G. Agostini, E. Borfecchia, D. Gianolio, A. Piovano, E. Gallo, C. Lamberti, *J. Phys. D* **2013**, *46*, 423001.
[21] P. Glatzel, T.-C. Weng, K. Kvashnina, J. Swarbrick, M. Sikora, E. Gallo, N. Smolentsev, R. A. Mori, *J. Electron Spectrosc. Relat. Phenom.* **2013**, *188*, 17–25.
[22] C. Garino, E. Borfecchia, R. Gobetto, J. A. van Bokhoven, C. Lamberti, *Coord. Chem. Rev.* **2014**, *277–278*, 130–186.
[23] S. Nikitenko, A. M. Beale, A. M. J. van der Eerden, S. D. M. Jacques, O. Leynaud, M. G. O'Brien, D. Detollenaere, R. Kaptein, B. M. Weckhuysen, W. Bras, *J. Synchrotron Radiat.* **2008**, *15*, 632–640.
[24] R. van Silfhout, A. Kachatkou, E. Groppo, C. Lamberti, W. Bras, *J. Synchrotron Radiat.* **2014**, *21*, 401–408.
[25] I. Kim, M. C. Chung, H. K. Choi, J. H. Kim, S. I. Woo, *Stud. Surf. Sci. Catal.* **1990**, *56*, 323–343.
[26] P. Sobota, *Chem. Eur. J.* **2003**, *9*, 4854–4860.
[27] C. K. Jorgensen, *Halogen Chemistry, Vol. 1*, Academic Press, New York, **1967**.
[28] C. K. Jorgensen, *Prog. Inorg. Chem.* **1970**, *12*, 101–157.
[29] R. J. H. Clark, D. Lewis, D. J. Machin, R. S. Nyholm, *J. Chem. Soc.* **1963**, 379–387.
[30] R. J. H. Clark, *J. Chem. Soc.* **1964**, 417–425.
[31] G. R. Shulman, Y. Yafet, P. Eisenberger, W. E. Blumberg, *Proc. Natl. Acad. Sci. USA* **1976**, *73*, 1384–1388.
[32] G. Vlaic, J. C. J. Bart, W. Cavigiolo, A. Michalowicz in *EXAFS and Near Edge Structure* (Eds.: A. Bianconi, L. Incoccia, S. Stipcich), Springer, Berlin, **1983**, p. 307–309.
[33] T. Usami, S. Takayama, M. Yokoyama, *J. Polym. Sci.* **1985**, *23*, 427–432.
[34] F. Farges, G. E. Brown, Jr., J. J. Rehr, *Phys. Rev. B* **1997**, *56*, 1809–1819.
[35] J. C. Swarbrick, Y. Kvashnin, K. Schulte, K. Seenivasan, C. Lamberti, P. Glatzel, *Inorg. Chem.* **2010**, *49*, 8323–8332.
[36] E. Gallo, C. Lamberti, P. Glatzel, *Phys. Chem. Chem. Phys.* **2011**, *13*, 19409–19419.
[37] K. Seenivasan, E. Gallo, A. Piovano, J. G. Vitillo, A. Sommazzi, S. Bordiga, C. Lamberti, P. Glatzel, E. Groppo, *Dalton Trans.* **2013**, *42*, 12706–12713.
[38] A. A. da Silva Filho, M. D. M. Alves, J. H. Z. dos Santos, *J. Appl. Polym. Sci.* **2008**, *109*, 1675–1683.
[39] S. I. Troyanov, E. M. Snigireva, V. B. Rybakov, *Zh. Neorg. Khim.* **1991**, *36*, 1117–1123.
[40] I. Pollini, *Solid State Commun.* **1983**, *47*, 403–408.
[41] C. H. Maulet, J. N. Tothill, P. Strange, J. A. Wilson, *J. Phys. C* **1988**, *21*, 2153–2179.
[42] A. Léon, O. Kircher, J. Rothe, M. Fichtner, *J. Phys. Chem. B* **2004**, *108*, 16372–16376.
[43] U. Bergmann, C. R. Horne, T. J. Collins, J. M. Workman, S. P. Cramer, *Chem. Phys. Lett.* **1999**, *302*, 119–124.
[44] S. A. Pizarro, P. Glatzel, H. Visser, J. H. Robblee, G. Christou, U. Bergmann, V. K. Yachandra, *Phys. Chem. Chem. Phys.* **2004**, *6*, 4864–4870.
[45] E. Gallo, F. Bonino, J. C. Swarbrick, T. Petrenko, A. Piovano, S. Bordiga, D. Gianolio, E. Groppo, F. Neese, C. Lamberti, P. Glatzel, *ChemPhysChem* **2013**, *14*, 79–83.
[46] L. Sementa, M. D'Amore, V. Barone, V. Busico, M. Causa, *Phys. Chem. Chem. Phys.* **2009**, *11*, 11264–11275.
[47] ADF2013, SCM, Theoretical Chemistry, Vrije Universiteit, Amsterdam, The Netherlands, http://www.scm.com.
[48] G. te Velde, F. M. Bickelhaupt, E. J. Baerends, C. Fonseca Guerra, S. J. A. van Gisbergen, J. G. Snijders, T. Ziegler, *J. Comput. Chem.* **2001**, *22*, 931–967.
[49] J. P. Perdew, K. Burke, M. Ernzerhof, *Phys. Rev. Lett.* **1996**, *77*, 3865–3868.
[50] S. Grimme, J. Antony, S. Ehrlich, H. Krieg, *J. Chem. Phys.* **2010**, *132*, 154104.
[51] E. van Lenthe, E. J. Baerends, *J. Comput. Chem.* **2003**, *24*, 1142–1156.
[52] E. van Lenthe, A. Ehlers, E. J. Baerends, *J. Chem. Phys.* **1999**, *110*, 8943–8953.

Received: December 4, 2014
Published online on February 24, 2015